

COMPASS: A Formal Framework and Aggregate Dataset for Generalized Surgical Procedure Modeling

Kay Hutchinson, *Member, IEEE*, Ian Reyes, Zongyu Li, *Member, IEEE*, and Homa Alemzadeh, *Member, IEEE*

Abstract—Objective: We propose a formal framework for modeling surgical tasks using a unified set of motion primitives (MPs) as the basic surgical actions to enable more objective labeling, aggregation of different datasets, and training generalized models for surgical action recognition.

Methods: We use our framework to create the Context and Motion Primitive Aggregate Surgical Set (COMPASS), including six dry-lab surgical tasks from three publicly-available datasets (JIGSAWS, DESK, and ROSMA) with kinematic and video data and context and MP labels. Methods for labeling surgical context and automatic translation to MPs are presented. We propose the Leave-One-Task-Out (LOTO) cross validation method to evaluate a model's ability to generalize to an unseen task.

Results: Our context labeling method achieves near-perfect agreement between consensus labels from crowd-sourcing and expert surgeons. Segmentation of tasks to MPs enables the generation of separate left and right transcripts and significantly improves LOTO performance. We find that MP recognition models perform best if trained on tasks with the same context and/or tasks from the same dataset.

Conclusion: The proposed framework enables high quality labeling of surgical data based on context and fine-grained MPs. Modeling surgical tasks with MPs enables the aggregation of different datasets for training action recognition models that can generalize better to unseen tasks than models trained at the gesture level.

Significance: Our formal framework and aggregate dataset can support the development of models and algorithms for surgical process analysis, skill assessment, error detection, and autonomy.

Index Terms—robotic surgery, surgical context, surgical gesture recognition, surgical process modeling, machine learning

This work was partially supported by the Engineering-in-Medicine center at the University of Virginia and by the National Science Foundation under Grant No. 1842490 and 2146295.

Kay Hutchinson led the development of the framework, methods, and models. Ian Reyes contributed to collecting and analyzing the dataset. Zongyu Li assisted in developing the TCN model. Homa Alemzadeh participated in developing and analyzing the framework and results.

Kay Hutchinson, Zongyu Li, and Homa Alemzadeh are with the Department of Electrical and Computer Engineering, University of Virginia, Charlottesville, VA 22903 USA ({kch4fk, zl7qw, ha4d}@virginia.edu)

Ian Reyes was with the Department of Computer Science, University of Virginia, Charlottesville, VA 22903 USA. He is now with IBM. (ir6mp@virginia.edu)

I. INTRODUCTION

Surgical gestures or surges are the building blocks of tasks and represent an important analytical unit for surgical process modeling [22], [31], skill assessment [38], [41], error detection [19], [26], [45], [46], and autonomy [15]. However, existing datasets and methods for gesture segmentation each use their own set of gesture definitions hindering direct comparisons between them and limiting their compatibility for combined analysis [4]. In addition, the descriptive gesture definitions are often subjective, and manual labeling of gestures is tedious and inconsistent. A recent survey of the state-of-the-art research on surgical gesture recognition [4] highlighted the need for a common surgical language with defined segmentation boundaries, as well as larger datasets to support comparative analysis and future work in error detection and prediction.

There are many datasets from real surgical tasks, but they only contain video data and are predominantly used for tool and object recognition such as those used for the EndoVis challenge [2]. Datasets with both kinematic and video data from a surgical robot are small and contain only a handful of trials of a few simulated or dry-lab tasks performed by a limited number of subjects. This hinders analysis and the training of machine learning (ML) models especially in the areas of surgical process modeling, gesture recognition, autonomy, and error detection. This scarcity of data also means ML models will see subjects, trials, and tasks that could be very different from their training set when they are deployed.

The most commonly used dataset for training and evaluation of different gesture recognition models is JIGSAWS [12] which contains kinematic data, videos, gesture labels, and surgical skill scores for three dry-lab surgical tasks. However, only two of its tasks, Suturing and Needle Passing, are labeled with similar sets of gestures; Knot Tying only shares the same first and last gestures with the other tasks. In addition, recent studies have indicated inconsistency and imprecise boundaries in the gesture labels. For example, [5] made 12 amendments to the gesture labels and [19] identified a significant discrepancy between the the beginning of G3 gestures in Suturing compared to Needle Passing while noting that the driving motion of G3 is important for distinguishing between normal and erroneous examples of this gesture. Furthermore, all subjects

have been right handed and gesture labels cannot be divided into actions performed by the left and right hands separately to allow for bimanual coordination assessments and analysis such as in [6].

Recent works in gesture recognition have each defined their own sets of gestures for their own datasets [8], [9], [16], [17], [30] with limited overlap between gestures. Action triplets [25], [29], [32] have also been proposed and consider tools and objects involved, but the combinations of verbs, instruments, and targets for action triplets can grow exponentially compared to a more limited number of gestures based on descriptive definitions. These works consider verb recognition separately from recognition of the full action triplet and use only video data. In comparison, we focus on verb recognition using only kinematic data since the tools and objects would need to be inferred from image data. This method would be helpful when image data is noisy and can be used to develop future models that fuse both kinematic and video data. Another recent work modeled surgical processes using statecharts with surgemes and triggers [10]. Related work on gestures and actions with label definitions are presented in Section IV and Tables VII and VIII. In all these works, the granularity of the actions can vary from the sub-gesture to the task level (see Figure 1).

Yet, there is still no formal framework that defines a standard set of surgical actions and their relations to gestures and tasks, which would enable direct comparisons between these works, their datasets, and their recognition models.

Our contributions are as follows:

- We propose a novel formal framework for modeling surgical tasks as a standardized set of motion primitives whose execution results in changes in important state variables that make up the surgical context. In this framework, surgical context characterizes the physical interactions among surgical objects and instruments and motion primitives represent the basic surgical actions across different surgical tasks and procedures.
- We develop a method for labeling surgical context from video data that achieves near-perfect agreement between crowd-sourced labels and expert surgeon labels, higher agreement among annotators than existing gesture definitions, and such that the context labels can be automatically translated into motion primitive labels.
- We apply our framework and labeling method to create an aggregate dataset, called COMPASS (Context and Motion Primitive Aggregate Surgical Set), consisting of kinematic and video data as well as context and motion primitive labels for a total of six dry-lab tasks from the JIGSAWS [12], DESK [17], and ROSMA [35] datasets.
- We introduce the Leave-One-Task-Out (LOTO) cross validation method to measure the ability of a recognition model to generalize to an unseen task since current datasets do not include all of the surgical tasks that a model may see when it is deployed.
- We perform the first evaluation of a surgical action recognition model trained on multiple tasks with data combined from different datasets by comparing model performance using the existing LOUO method as well as our proposed LOTO cross validation method.

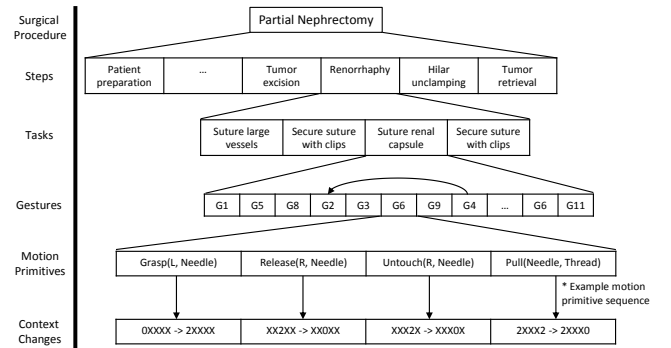


Fig. 1: Surgical Hierarchy. Adapted from [19]

The tools for labeling surgical context based on video data and automated translation of context labels to motion primitives as well as the aggregated dataset with context and motion primitive labels are made publicly available at <https://github.com/UVA-DSA/COMPASS> to facilitate further research and collaboration in this area.

II. METHODS

Our framework models surgical procedures as a language with a grammar dictating how motion primitives are combined to perform gestures and tasks, thus bridging the gap between semantic-less motions described by [31] and [22], and intent-based gestures described by [27]. In our framework, we formally define surgical motion primitives, how they relate to surgical context and task progress, and how they can be combined to perform both gestures and tasks. To accomplish this, we develop an objective method for labeling surgical context and apply it to three publicly available datasets to create the COMPASS aggregated dataset. Then, we train an action recognition model and evaluate its performance under new and existing cross validation methods.

A. Framework

1) *Surgical Hierarchy*: Surgical procedures follow the hierarchy of levels defined in [31] which provides context [45] for actions during the procedure, as shown in Figure 1. A surgical **operation** can involve multiple **procedures** which are divided into **steps**. Each **step** is subdivided into **tasks** comprised of **gestures** (also called sub-tasks or surgemes). These **gestures** are made of basic **motion primitives** such as moving an instrument or closing the graspers which effect changes in important states in the surgical **context**.

2) *Surgical Context*: A surgical environment (either during dry-lab or real surgical procedures) can be modeled by a set of state variables that characterize the status and interactions among surgical instruments (e.g., graspers, scissors, electro-cautery) and objects (e.g., needles, threads, blocks, balls, sleeves, rings) or anatomical structures (e.g., organs, tissues, tumors) in the physical environment. Changes in the surgical context happen as the result of performing a set of basic motion primitives by the robot (either controlled by the surgeon operator or autonomously). Figure 2a shows an example of the Needle Passing task modeled as a finite

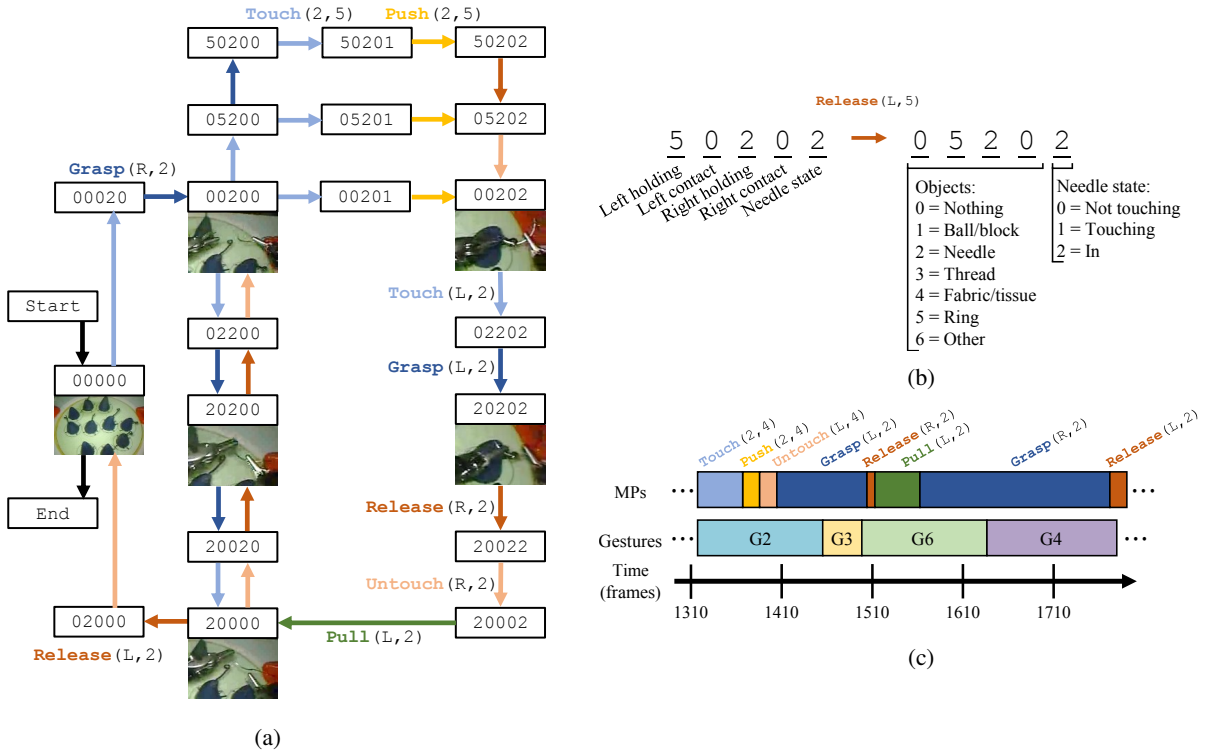


Fig. 2: Modeling the Needle Passing Task: 2a) Model of the ideal performance of a Needle Passing trial with context and MPs. 2b) An example of a motion primitive in Needle Passing showing the state variables, objects, and needle states. 2c) Example of alignment between MPs and gestures in a Needle Passing trial that also shows the discrepancy in the G3 boundary as noted by [19] where the 'Push' MP is not part of G3. From [12], G2: positioning needle, G3: pushing needle through tissue, G4: transferring needle from left to right, G6: pulling suture with left hand. Figure best viewed in color.

automata with the states representing the surgical context and the transitions representing the motion primitives. This new representation of surgical tasks enables the incorporation of surgical context into surgical procedure modeling which is missing from the previously proposed models such as grammar graphs and Hidden Markov models [1] where lower level actions are obscured by hidden states.

We define the surgical context using two sets of variables that can be observed or measured using kinematic and/or video data from a surgical scene: (i) general state variables relating to the contact and hold interactions between the tools and objects in the environment, and (ii) task-specific state variables describing the states of objects critical to the current task. We also define independent state variables for the left and right tools to enable the generation of separate label sets to support side-specific skill assessment, hand coordination analysis, and improved MP recognition. There are four general state variables as shown in Figure 2b. An additional task-specific state variable is appended to the right of the general context variables to describe progress in the task. For Suturing and Needle Passing, the needle, if held, can be “not touching”, “touching”, or “in” the fabric or ring. For Knot Tying, the thread can be “wrapped” around the opposite grasper, in a “loose” knot, or in a “tight” knot. For Peg Transfer and Post and Sleeve, the block can be “on” or “off” the peg. For Pea on a Peg, the pea, if held, can be “in the cup”, “stuck to other peas”, “not stuck to other peas”, or “on the peg”. For example, in Figure 2b, the state 50202 indicates that the left grasper is

holding a ring, the right grasper is holding the needle, and the needle is in the ring.

3) Motion Primitives: We define a unified set of six modular and programmable surgical motion primitives (MPs) to model the basic surgical actions that lead to changes in the physical context. As shown in Equation 1, each MP is characterized by its type (e.g., grasp), the specific tool which is used (e.g., left grasper), the object with which the tool interacts (e.g., block), and a set of constraints that define the functional (e.g., differential equations characterizing typical trajectory [13]–[15]) and safety requirements (e.g., virtual fixtures and no-go zones [7], [37]) for the execution of the MPs:

$$MP(tool, object, constraints) \quad (1)$$

In this framework, tools and objects are considered classes as in object-oriented programming and can have attributes such as the specific type of tool and current position. Also, the MPs can be further decomposed into the fundamental transformations of move/translate, rotate, and open/close graspers which characterize the low level kinematic commands for the programming and execution of motions on a robot, but we do not examine that level here.

Our MPs are similar to the recently proposed action triplets in [32] for surgical activity recognition based on video data in real surgical tasks. But we focus on developing and applying standardized labels to dry-lab datasets with both kinematic and video data to enable comparative analyses between datasets and tasks. Kinematic data can support analysis for safety

TABLE I: General motion primitives for changes in context: 'L' and 'R' represent the left and right graspers as tools, 'a' is a generic object as listed in Fig 2b, and 'X' can be any value.

Motion Primitive	Context Change
Touch(L, a)	X0XX → XaXX
Touch(R, a)	XXX0 → XXXa
Grasp(L, a)	0aXX → aXXX
Grasp(R, a)	XX0a → XXaX
Release(L, a)	aXXX → 0aXX
Release(R, a)	XXaX → XX0a
Untouch(L, a)	XaXX → X0XX
Untouch(R, a)	XXXa → XXX0

and skill, and be used to develop dynamic motion primitives (DMPs) [14]. The COMPASS framework can be extended to real surgical procedures by adding additional tool-specific verbs similar to those proposed in [32] (e.g., "Cut" for scissors). Segmenting tasks into MPs allows the separation of actions performed by the left and right hands and the generation of separate sets of labels which supports skill analysis of bimanual coordination and surgical automation [4]. This enables more detailed skill assessment and analysis of bimanual coordination such as in [6]. To generate separate left and right label sets, MPs performed by each arm of the robot are split into new transcripts and the 'Idle' MP is used to fill the gaps created by the separation so that every kinematic sample has a label.

Table I shows the set of MPs and corresponding changes to surgical context applicable to all tasks. Table II shows the sets of MPs and corresponding changes to surgical context applied to specific dry-lab tasks in our aggregated dataset. In this work, we only focus on dry-lab tasks where the tools are graspers. We also do not model or analyze the MP-specific functional and safety constraints since we only focus on recognition and not automation or monitoring.

The definition of MPs based on the changes in the surgical context could enable the translation of context and MPs to existing gesture labels and facilitate aggregation of different datasets labeled with different gesture definitions. Figure 2c shows an example alignment between MPs and gestures in a Needle Passing trial from the JIGSAWS dataset. We will discuss the labeling of context and automatic translation from context labels to MPs in the next section. However, the automated translation from context and MP labels to existing gesture definitions is complicated, because of the possibility of executional and procedural errors as defined in [19], and is, thus, beyond the scope of this paper.

B. Labeling of Context and Motion Primitives

1) *Context Labeling:* Gesture recognition models using supervised learning require a large number of annotated video sequences [33]. However, manual labeling of gestures is time consuming and subjective which can lead to labeling errors [5]. To address this, we have developed a tool for manual annotation of the surgical context (states of the objects and instruments) based on video data and used it to label all trials in six tasks from the JIGSAWS, DESK, and ROSMA datasets.

Labeling video data for surgical context provides a more objective way of recognizing gestures and thus can lead to a higher level of agreement among annotators. Also, as noted in [21], labels for surgical workflow require guidance from surgeons while annotations for surgical instruments do not. Since context labels document the objects held by or in contact with the left and right graspers, they rely less on surgical knowledge than gestures which require anticipating the next actions in a task to mark when a gesture has ended. Figure 3 shows a snapshot of the tool for manual labeling of context based on video data.

To ensure reliable and high quality annotations, three full sets of context labels were obtained so that consensus and agreement could be taken among them. Two of the authors, with extensive experience with the datasets and the dry-lab robotic surgery tasks, each produced a full set of labels for all the trials. The third set of labels was crowd-sourced to engineering students. Consensus was taken using majority voting for each state variable. This set of labels is part of the COMPASS dataset and we refer to it as the "Consensus" set. A group of expert surgeons also labeled a set of six trials, one from each task, to evaluate the quality of the labels, and we refer to this set as the "Surgeon" set. In addition, a subset of trials in the JIGSAWS tasks were labeled by three independent annotators for context, MPs, and gestures to assess and compare the different labeling methods and the context to motion primitive translation. We refer to these labels as the "Multi-level" set.

TABLE II: Task-specific motion primitives for changes in context: 'L' and 'R' represent the left and right graspers as tools, objects are encoded as in Fig 2b, 'X' can be any value.

Motion Primitive	Context Change
Suturing/Needle Passing	
Touch(2, 4/5)	2XXX0 → 2XXX1
Touch(2, 4/5)	XX2X0 → XX2X1
Push(2, 4/5)	2XXX1 → 2XXX2
Push(2, 4/5)	XX2X1 → XX2X2
Pull(2, 3)	2XXX2 → 2XXX0
Pull(2, 3)	XX2X2 → XX2X0
Knot Tying	
Pull(L, 3)	3XXX0 ↔ 3XXX1
Pull(R, 3)	XX3X0 ↔ XX3X1
Pull(L, 3) Pull(R, 3)	3X3X1 → 3X3X2
Pull(L, 3) Pull(R, 3)	3X3X2 → 3X3X3
Peg Transfer and Post and Sleeve	
Touch(1, Post)	XXXX0 → XXXX1
Untouch(1, Post)	XXXX1 → XXXX0
Pea on a Peg	
Grasp(L, 1)	0XXX0 → 1XXX1
Grasp(R, 1)	XX0X0 → XX1X1
Pull(L, 1)	1XXX1 → 1XXX2
Pull(R, 1)	XX1X1 → XX1X2
Pull(L, 1)	1XXX1 → 1XXX3
Pull(R, 1)	XX1X1 → XX1X3
Touch(1, 1)	XXXX3 → XXXX2
Untouch(1, 1)	XXXX2 → XXXX3
Touch(1, Peg)	XXXX3 → XXXX4
Untouch(1, Peg)	XXXX4 → XXXX3
Release(L, 1)	1XXXa → 0XXX0
Release(R, 1)	XX1Xa → XX0X0
Push(L, 1)	1XXX2 → 1XXX1
Push(R, 1)	XX1X2 → XX1X1

2) *Context to Motion Primitive Translation*: The context labels are translated automatically into MP labels using the MP definitions presented in Tables I and II. Using these tables, if multiple states changed between labeled frames, then a Grasp would have a higher priority than a Touch and a Release would have a higher priority than an Untouch, if they were performed on the same object by the same tool. Otherwise, all MPs were listed in the MP transcript so that separate MP transcripts for the left and right sides could be generated. Context labels are provided at 3 Hz and the context to MP translation assumes that states persist until the next context label in order to generate an MP label for each kinematic sample at 30 Hz.

C. COMPASS Dataset

As shown in Figure 4, the COMPASS dataset contains 39 trials of Suturing (S), 28 trials of Needle Passing (NP), and 36 trials of Knot Tying (KT) performed by eight subjects from the JIGSAWS dataset; 47 trials of Peg Transfer (PT) performed by eight subjects from the DESK dataset; and 65 trials of Post and Sleeve (PaS), and 71 trials of Pea on a Peg (PoaP) performed by 12 subjects from the ROSMA dataset. Videos are at 30 fps for the stereoscopic JIGSAWS and DESK tasks and 15 fps for the single camera for the ROSMA tasks. The kinematic data have been downsampled to 30 Hz and contain position, velocity, orientation (in quaternions), and gripper angle variables. Since linear velocity data was not available for all tasks, it was derived from the position data using a rolling average over five samples. The ROSMA dataset did not contain gripper angle, so a separate round of manually labeling video data was performed to approximate the gripper angle as open or closed. To uniquely identify each individual file, a naming system that includes the task, subject number, and trial number was applied to facilitate matching kinematic, video, and label files. For example, the name *Pea_on_a_Peg_S02_T05* identifies



Fig. 3: App for Context Labeling based on Video Data

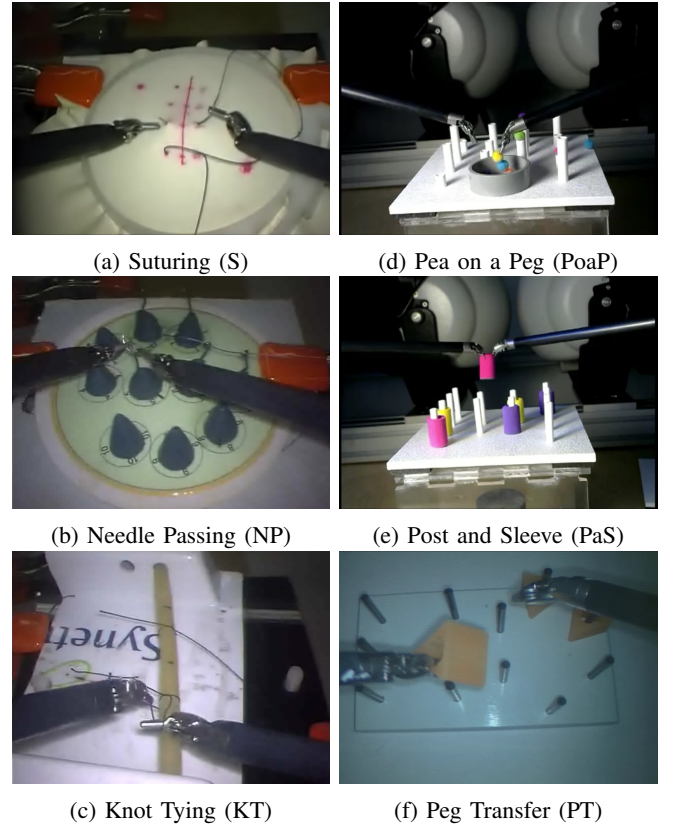


Fig. 4: Tasks included in the COMPASS dataset: Suturing (S), Needle Passing (NP), and Knot Tying (KT) from the JIGSAWS dataset [12]; Pea on a Peg (PoaP) and Post and Sleeve (PaS) from the ROSMA dataset [35]; and Peg Transfer (PT) from the DESK dataset [17].

the fifth trial of Pea on a Peg performed by subject two.

The COMPASS dataset also includes consensus context labels at 3 Hz and automatically generated motion primitive labels interpolated to 30 Hz for both arms of the robot so that every kinematic sample has an MP label. The original gesture labels from JIGSAWS and DESK datasets are synced and renamed under the new naming convention and included to promote comparisons between data and label sets.

D. Gesture and Motion Primitive Recognition

Surgical gesture recognition is a critical component of surgical process modeling [22], [31], skill assessment [11], [43], error detection [19], [26], [45], and autonomy [8]. Much work has been done in developing models for gesture recognition mostly using data from the Suturing task in the JIGSAWS dataset as summarized in [4]. Previous works [45] and [4] have provided baseline gesture recognition model accuracies for various methods including LSTM [45], TCN [24], SDSDL [36], and SC-CRF [23] that were trained and evaluated on the JIGSAWS dataset using only patient-side kinematic data. The SDSDL and SC-CRF models provide baseline accuracies for state-of-the-art models in Table V. However, existing gesture recognition models have been task-specific, so we introduce MPs and the LOTO cross validation setup to improve and assess a model's ability to generalize to an unseen task by leveraging data from other tasks. Our models predict just the

verb of the MP using only kinematic data and could thus be compared to the results of action triplet recognition models [25], [32] that also predict just the verb but use video data.

1) Temporal Convolutional Network (TCN) Implementation:

One of the fastest and best performing models that used only kinematic data for gesture recognition in [4] was the Temporal Convolutional Network (TCN). We adopt the TCN model from [24] for action recognition and compare its performance in terms of accuracy and edit score for motion primitives and gestures under the LOUO and LOTO cross validation setups. This model has an encoder-decoder structure, each consisting of three convolutional layers with pooling, channel normalization, and upsampling. As in [24], the kernel size is set to the average duration of the shortest action class (e.g., gesture or MP), the stride is 1, and the three layers have 32, 64, and 96 filters respectively. The loss function is cross-entropy and the model was trained using the Adam optimizer [20]. The input signal to the model is the time-series kinematic data, x_t , and the output is a class label, y_t , for each time-series sample. Experiments were performed on a computer with an Intel Core i9 CPU @ 3.60GHz x 16 and 64GB RAM, running Linux Ubuntu 18.04 LTS, and an NVIDIA GeForce RTX 2070 GPU running CUDA 10.2, and the models were built and trained using Torch 1.10.1 [34].

Experimentation with different combinations of kinematic variables as inputs to the TCN revealed that using only the position, linear velocity, and gripper angle resulted in the best performance. This is consistent with the best performing gesture recognition models that relied on kinematic data as reported in [4].

The learning rate and weight decay hyperparameters for all TCN models were selected based on a grid search of values by training on the JIGSAWS dataset with gesture labels for each cross validation setup. For LOUO models, the learning rate was 0.00005 and the weight decay was 0.0005. For LOTO models, the learning rate was 0.0001 and the weight decay was 0.001. These values were fixed for all models of their respective cross validation setup so that the effect of different training and label sets on model performance could be analyzed.

We compare the performance of the TCN when trained with four different sets of labels: gestures, MPs for only the left side (Left MPs), MPs for only the right side (Right MPs), and MPs for both sides together (MPs).

2) Cross Validation Setups: The models were evaluated using two cross validation setups: Leave-One-User-Out (LOUO) from [1] and our novel Leave-One-Task-Out (LOTO). Since tasks from different datasets did not share the same subjects, the LOUO setup was extended to include the new subjects resulting in a maximum of 28 folds (corresponding to 28 users) when the model was trained on data from all tasks. Note that LOUO is used over the Leave-One-Supertrial-Out (LOSO) method in comparing gesture recognition models as it measures a model's ability to generalize to an unseen user which is expected of a deployed model [4].

In the LOTO setup, all of the data for one task was held out as the test set while the model was trained on all of the data for a set of other tasks. Similar to the existing LOSO and LOUO

setups, average accuracy and edit score across the folds can be reported and used to compare models. However, examining each fold's performance and considering the relationship and similarity between the tasks in the training and test sets yields insights about the generalizability of the model to unseen tasks and the data needed to train a model.

Data from different tasks was grouped together if they shared the same context states, to improve the variability and size of training data. In the COMPASS dataset, there were two possible combinations: S + NP = 'SNP' where both tasks have a task-specific needle state, and PT + PaS = 'PTPaS' where both tasks have a task-specific block state. Tasks could also be grouped together if they come from the same dataset: S + NP + KT = 'JIGSAWS' and PaS + PoaP = 'ROSMA'. We also train a model by combining all of the data, referred to as 'All'. We also considered specific combinations of training data that tested on one task but removed the contextually similar tasks, as defined above, from the training set to assess the importance of augmenting the training set with data from similar tasks.

E. Evaluation Metrics

1) Context Labeling: We verify the quality of the context labels by calculating the agreement between context labels from the surgeons and consensus context labels from the annotators using Krippendorff's Alpha [33]. This metric considers the probability D_e that two labelers produced the same annotation due to chance rather than agreement on the data to label, and the observed disagreement D_o between each labeler's annotations. Then, Krippendorff's Alpha is calculated using Equation 2:

$$\alpha = 1 - \frac{D_o}{D_e} \quad (2)$$

The coefficient α is a value ranging from 1 to -1, with $\alpha > 0.8$ indicating near-perfect agreement, a value between 0.6 and 0.8 indicating substantial agreement, and smaller values indicating less agreement. $\alpha = 0$ indicates no agreement other than by chance and negative values reflect more pronounced disagreement. There are different versions of Krippendorff's Alpha for specific kinds of annotations. Each of the labelers annotated a sequence of states encoded as numbers. The annotations do not have numerical significance and can best be described as categorical data, so the nominal distance or difference function is best suited to quantify the agreement between labelers annotating for context. The nominal distance or difference function in Equation 3 is used to calculate to calculate both D_e and D_o [18] as given in Equation 4 where n_l is the number of labelers and n_u is the total number of frames which two or more labelers annotated.

$$d_{nominal}(\text{label}_1 \text{ label}_2) = \begin{cases} 0 & \text{if label}_1 = \text{label}_2 \\ 1 & \text{if label}_1 \neq \text{label}_2 \end{cases} \quad (3)$$

$$D_o = \frac{1}{2n_u n_l (n_l - 1)} \sum_{l_1, l_2 \in \text{all labels}} d_{nom}(l_1, l_2) \quad (4)$$

$$D_e = \frac{1}{2n_u n_l (n_u n_l - 1)} \sum_{l_1, l_2 \in \text{all labels}} d_{nom}(l_1, l_2)$$

2) *Context to Motion Primitive Translation and Gesture and Motion Primitive Recognition*: We use the following standard metrics for evaluation and comparison of the context to motion primitive translation and gesture and motion primitive recognition models.

Accuracy: Given the lists of predicted and ground truth labels, the accuracy is the ratio of correctly classified samples divided by the total number of samples in a trial.

Edit Score: We report the edit score as defined in [24] which uses the normalized Levenshtein edit distance, $edit(G, P)$, by calculating the number of insertions, deletions, and replacements needed to transform the sequence of predicted labels P to match the ground truth sequence of labels G . The edit score is normalized by the maximum length of the predicted and ground truth sequences and is thus computed using Equation 5 where 100 is the best and 0 is the worst.

$$\text{Edit Score} = (1 - \frac{edit(G, P)}{\max(len(G), len(P))}) \times 100 \quad (5)$$

III. RESULTS

A. Labeling Agreement

We use Krippendorff’s Alpha to measure agreement on the context labels from annotators as well as the agreement between the consensus context labels from annotators (“Consensus”) and the labels from expert surgeons (“Surgeon”). In addition, three new annotators labeled context, MPs, and gestures (“Multi-level”) for the same subset of trials in the S, NP, and KT to compare labeling methods.

1) *Consensus compared to expert surgeons and JIGSAWS*: The third column in Table III shows the Krippendorff’s Alpha between Consensus and Surgeon context labels. We find that all tasks had an α of at least 0.8 and the average for all tasks (weighted for the number of frames for each task) was 0.92, indicating near-perfect agreement between crowd-sourced context labels and those given by surgeons.

On the other hand, the α between the Multi-level context and Surgeon context labels were 0.86, 0.90, and 0.89, respectively. But the α between Multi-level gesture and JIGSAWS gesture labels from the same annotators were only 0.34, 0.04, and 0.06, respectively. This shows that there much higher agreement when labeling for context than for gestures and the existing JIGSAWS labels are difficult to reproduce. We find that crowd-sourcing context labels results in high quality annotations which are comparable to those given by expert surgeons.

2) *Labeling Agreement using Context, MPs, and Gestures*: The second column in Table III shows the agreement among crowd-sourced annotators, measured using the average Krippendorff’s Alpha, for each task where in four we see a near-perfect agreement (α above 0.8) and in two substantial agreement (α at least 0.6). The average for all tasks was 0.84, weighted for the number of frames for each task, indicating substantial agreement in labeling overall. We note that long segments of near-perfect agreement are punctuated by disagreements at the transitions between context. However, disagreement is limited to a few context states instead of the

TABLE III: Krippendorff’s Alpha among annotators and between Consensus and Surgeon context labels.

Task	Among annotators	Between Consensus and Surgeon
Suturing	0.69	0.86
Needle Passing	0.85	0.90
Knot Tying	0.79	0.94
Peg Transfer	0.90	0.94
Pea on a Peg	0.83	0.93
Post and Sleeve	0.89	0.97

gesture label for a specific frame which results in much greater agreement between annotators when labeling for context than for gestures. Then, consensus obtained by majority voting for each state variable separately results in a high quality set of fine grained labels.

When the three independent annotators labeled the S, NP, and KT trials for context, MPs, and gestures (“Multi-level”), the α among annotators were, respectively, 0.72, 0.91, and 0.89 for context; 0.33, 0.41, and 0.26 for MPs; and 0.24, 0.08, and 0.20 for gestures. This shows that there is the least agreement when labeling using the descriptive gesture definitions, but labeling MPs directly is also difficult, likely due to their short durations. Annotating for context has the greatest agreement since labels are based on well-defined interactions among surgical tools and objects that can be observed in video data.

B. Context to Motion Primitive Translation

The context to MP translation allows us to leverage the high quality context labels in creating surgical workflow annotations and aggregating different surgical datasets. To assess the performance of this step, we translate the context labels in the “Multi-level” annotations set and compare the resulting translated MP transcripts to the ground truth MP labels for each annotator. We calculate the accuracy and edit score for each task between ground truth and translated MPs.

The input context labels show variability by the type of task (S, NP, KT) and by the skill of the annotator, both of which can affect the resulting translated MP labels. So we first used the agreement scores with the “Surgeon” context labels set and JIGSAWS gesture labels as a measure to assess the quality of each annotator and found appreciable differences in the accuracy of each annotator. The accuracies for annotators 1, 2, and 3 were, respectively, 0.58, 0.69, and 0.71 when labeling for context (compared to surgeons), and 0.27, 0.35, and 0.65 when labeling for gestures (compared to JIGSAWS). Thus, annotator 3 was the most reliable annotator overall, but annotator 2 was almost as reliable for context labels. We also found that the annotators had similar agreement with surgeons for NP which is consistent with the results in Table III.

TABLE IV: Accuracy and edit score between consensus ground truth and translated motion primitives for Multi-level labels.

Task	Annotator 1 (Acc/Edit Score)		Annotator 2 (Acc/Edit Score)		Annotator 3 (Acc/Edit Score)	
S	0.27	33.9	0.18	26.9	0.23	30.1
NP	0.64	67.4	0.27	45.1	0.45	46.4
KT	0.50	53.8	0.31	56.1	0.53	56.8

TABLE V: TCN model accuracies and edit scores for gestures under the LOUO cross validation setup compared to state-of-the-art models. Note that results for state-of-the-art models were only available for the tasks from the JIGSAWS dataset.

Tasks	Gestures		Baseline Accuracies (%)	
	Acc (%)	Edit Score	SDSDL [36]	SC-CRF [23]
PT	55.0	69.7		
S	83.8	83.5	86.3	85.2
NP	73.4	81.5	74.9	77.5
KT	83.4	84.5	82.5	80.6
SNP	77.8	81.7		
JIGSAWS	78.5	79.7		

As shown in Table IV, the translation script can better translate motion primitives for annotators 1 and 3 compared to annotator 2. Also the task breakdown reveals inter-rater variability across tasks, with highest edit score for annotator 1 on S and NP tasks and for annotator 3 on KT. However, the ground truth MP labels used in this evaluation had very low agreement among annotators compared to context labels and assessing their reliability is beyond the scope of this paper. Future work will collaborate with surgeons for high quality annotations using multi-level labeling methods so we can better evaluate these different methods and improve the automated translation between them.

C. Gesture and Motion Primitive Recognition

In this section we present the performance of TCN models in recognizing gestures and motion primitives in comparison to the state-of-the-art models and with different combinations of training and testing sets. Using MP labels, different datasets can be combined and models trained on them can be compared. We show the limitations of using gestures when using a model to predict on an unseen task in the LOTO setup and how using MPs can help overcome this challenge. Note that a direct performance comparison between the models for recognizing gestures vs. motion primitives is not reasonable since they are at different levels of the surgical hierarchy.

1) *LOUO*: Table V compares the accuracies and edit scores averaged over the folds of the LOUO setup for the TCN models trained to recognize gestures and Figure 5 shows the results for the MP models. Accuracies for two state-of-the-art models are also presented in Table V against which our TCN model performs comparably. The TCN performed best on the Suturing task alone achieving an accuracy of 83.3% and an edit score of 83.5 which is slightly better than the 79.6% accuracy and 85.8 edit score reported by [24].

We also observe that although the Suturing and Needle Passing tasks are contextually similar in the COMPASS framework and share the same gesture labels in the JIGSAWS dataset, the TCN exhibits a 10% decrease in accuracy in recognizing gestures in Needle Passing compared to Suturing. And, despite Knot Tying only sharing two similar gestures and having a different task-specific context state than the other two JIGSAWS tasks, the TCN’s performance on KT is comparable to its performance on S. When data from multiple tasks is combined for the ‘SNP’ and ‘JIGSAWS’ models, the TCN

model’s accuracy is only about the average of its performance on individual tasks while the edit score for the JIGSAWS model drops to 79.7 which is lower than for any single task in that dataset. Thus, there does not appear to be a benefit to combining data from the JIGSAWS tasks at the gesture level. The Pea on a Peg (PoaP) and Post and Sleeve (PaS) tasks from the ROSMA dataset did not have gesture labels, so no gesture recognition models were trained for them. The Peg Transfer (PT) task of the DESK dataset did have gesture labels although their definitions were much closer in scope to MPs rather than the more complex gestures of the JIGSAWS dataset. The TCN only achieves an accuracy of 55.0% for gesture recognition on the PT task which is comparably lower than its performance for any of the MP recognition models. This suggests that the level of the labels in the surgical hierarchy has an impact on action recognition performance so it is difficult to directly compare recognition models trained on labels of different granularities.

By examining Figure 5, we note that MP recognition performance is better for tasks in the ROSMA dataset, and to a somewhat lesser extent for the DESK dataset, than for tasks in the JIGSAWS dataset. This could be because the tasks in the JIGSAWS dataset are more complex since they have more complex grammar graphs while tasks in the ROSMA and DESK datasets are variations on a pick and place task with simpler task grammar graphs. This is supported by the higher edit scores for the models trained for the ROSMA and DESK datasets while the models for the JIGSAWS dataset have lower edit scores. Furthermore, although combining data at the MP level also resulted in performance metrics that are about the average of the individual tasks that were combined, training separate models for each side of the robot always resulted in higher accuracies with comparable or better edit scores. So, having separate annotations and models for the left and right arms of the robot improves MP recognition performance.

2) *LOTO*: Although performance metrics have been reported as the average across all the folds in the LOSO or

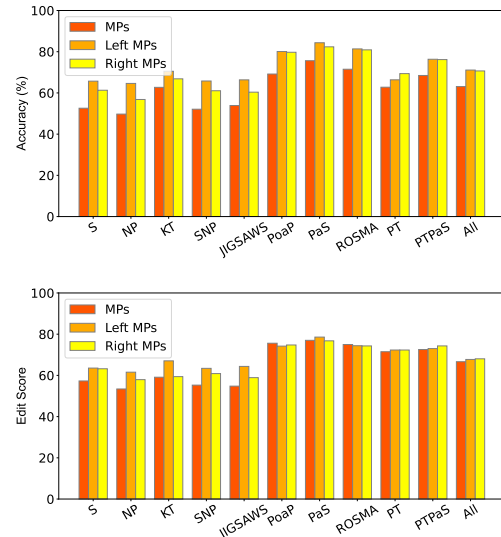


Fig. 5: TCN model accuracies and edit scores for MPs under the LOUO cross validation setup.

TABLE VI: TCN model accuracies and edit scores for MPs and gestures under the LOTO cross validation setup.

Test Set	Training Set (Task combinations)					Gestures (Acc/Edit Score)		MPs (Acc/Edit Score)		Left MPs (Acc/Edit Score)		Right MPs (Acc/Edit Score)	
S	NP	KT	PT	PaS	PoaP	24.4	33.9	43.2	48.3	56.2	52.7	46.3	48.2
S													
S													
S													
NP	S	KT	PT	PaS	PoaP	28.8	38.2	37.2	46.9	49.9	52.8	44.7	48.3
NP													
NP													
NP													
KT	S	NP	PT	PaS	PoaP	6.8	9.3	29.7	40.5	48.1	50.4	34.5	42.8
KT													
KT													
KT													
PT	S	NP	KT	PaS	PoaP	59.3	65.0	59.3	57.3	61.2	57.3	61.2	57.3
PT													
PT													
PT													
PaS	S	NP	KT	PT	PoaP	61.2	66.0	62.3	58.0	63.7	59.9	63.7	59.9
PaS													
PaS													
PaS													
PoaP	S	NP	KT	PT	PaS	56.2	41.8	44.9	55.7	41.0	51.9	41.0	51.9
PoaP													
PoaP													
PoaP													
PoaP	S	NP	KT	PT	PaS	53.5	62.9	59.3	48.3	57.1	43.8	57.1	43.8
PoaP													
PoaP													
PoaP													

LOUO setups, examining the results of individual folds in the LOTO setup can yield important insights about the ability of the model to generalize to an unseen task. This is important to analyze since datasets available for training ML models are limited in size and variety, so a deployed model will likely see tasks not represented in its training data.

Table VI reports the accuracies and edit scores for different folds of models from the LOTO setup and immediately shows the limitations of existing gesture definitions. Note that only the JIGSAWS dataset had gesture labels that could be used in the LOTO setup, so gesture recognition models using tasks from different datasets could not be trained because gesture labels were not present or were not compatible. A gesture recognition model trained on S or NP is able to transfer to NP or S respectively, but when KT is added to the training set, performance is severely decreased: a model tested on S drops from an accuracy of 48.5% to 24.4%, and a model tested on NP drops from 37.9% to 28.8% when KT is added to the training set. This is due to the lack of generalizable gesture labels between these tasks since S and NP have an almost completely different set of gestures than KT. Thus, gesture recognition for the KT task using a model trained on S and NP is particularly poor with an accuracy of only 6.8%. Hence, at the gesture level, combining data from different tasks is not beneficial for a model that must predict on an unseen task.

Comparatively, when MPs are used, the model is able to predict on a new task like KT by leveraging information learned from other tasks that are dissimilar to it such as S and NP. Adding data from a dissimilar task has a much smaller detrimental effect at the MP level than at the gesture level. For example, the model's accuracy drops less than 1% for S and less than 5% for NP when KT is added to the training set.

When the model must predict MPs on a dissimilar task with

a different task-specific context state then combining data from all available tasks does best. KT improves from an accuracy of 29.7% to 32.7% and PoaP improves from 53.5% to 56.3% by including data from other datasets.

Splitting the MP labels into separate transcripts and training separate models for the left and right arms of the robot results in significant improvements compared to having a single model. We find that combining similar tasks based on having the same task-specific context state, namely S with NP and PT with PaS, usually results in models with higher accuracies than combining data from all tasks together. The exception is PaS where the Left MP model has the best performance when PT is not included in the training set and the Right MP model is trained on only PT and PoaP. Notably, for PaS, combining both a similar task, PT, and a task from the same original dataset, PoaP, results in the best performance for the Right MP model which suggests that there may be a benefit to including data from the same subject even if the task is dissimilar. Likewise, the model also performs best when trained on a task that is both similar and from the same dataset, specifically training on S and testing on NP and vice versa. This means that including a similar task by the same subject or subjects enables the model to generalize better to an unseen task. With separate models for the left and right sides, if a similar task is not present, as for KT and PoaP, then including only data from the same original dataset does best. This suggests that having data from the same subjects but different tasks is more important than data from different tasks and different subjects in helping the model generalize to an unseen task.

IV. RELATED WORK

Surgical Workflow Segmentation: This work fits within the broader goal of understanding and modeling the surgical

scene and processes. Surgical workflow segmentation can be done at different levels of granularity such as phases, steps, tasks, and actions [39], [40], [42], [44]. In this work, we focus on the gesture and action (MP) levels and extend the surgical hierarchy to include context.

Surgical Gesture Recognition: Much work in surgical gesture recognition has been based on the JIGSAWS dataset [12] and the “Language of Surgery” project [27] where surgical procedures are modeled as a language and a grammar dictates how gestures are combined to perform tasks. Gestures are defined as “the smallest surgical motion gesture that encapsulates a specific intent, (e.g., insert needle through tissue)” with semantic meaning. Recent works have introduced new models and datasets, as summarized in Table VII but differing gesture definitions limit comparisons between them as well as their generalizability to other tasks. Specifically, [9], [30], and [16] all performed gesture recognition based on kinematic data, but used different datasets and gesture definitions making comparisons difficult. Nor did they combine data from multiple sets since the gesture labels are incompatible.

Surgical Actions Motions, motion primitives, actions, and action triplets are all used to refer to the level of the surgical hierarchy below gestures. In surgical process modeling, [31] and [22] define motions as an activity performed by only one hand and without semantic meaning. Many other works, including this one, define actions as atomic units as listed in Table VIII. An early work [11] used separate actions for the left and right arms of the robot for skill assessment given sequences of those actions, but did not perform action recognition. Since then, action recognition models have been developed, but mainly use video data. These have been supported by the many datasets for surgical tool and object recognition challenges such as [3] and [2] using videos and images from real surgery. For example, using the EndoVis 2019 dataset, [42] summarizes the performance of action recognition models from a competition, but only considered four different actions and concluded that larger datasets are needed to improve models for this purpose. Applications of action recognition include creating an autonomous assistant [8]. More recently, [32] and [25] both perform action triplet recognition on video data from real surgeries, but still use different sets of actions. In addition, combinations of these verbs, instruments, and targets grew very large and had to be limited or grouped to reduce the total number of possible classes. They also do not formally model how actions comprise surgical tasks which would be beneficial for surgical process modeling, skill assessment, and error detection. In our framework, we formally define motion primitives, how they relate to surgical context and task progress, and how they can be combined to perform tasks.

V. DISCUSSION AND CONCLUSION

In summary, we present a framework for modeling surgical tasks as motion primitives that cause changes in surgical context and apply it to three publicly available datasets to create an aggregate dataset of kinematic and video data along with context and motion primitive labels. Our method for labeling context achieves substantial to near-perfect agreement

between annotators and expert surgeons. We introduce the leave-one-task-out (LOTO) cross validation setup, and perform the first evaluation of a surgical action recognition model in terms of its ability to generalize to an unseen task. Using motion primitives, we combine data from different datasets, tasks, and subjects and find that having separate models for the left and right sides improves performance. Specifically, we find that the models perform best for an unseen task if trained on data from a task with the same context states in combination with data from tasks in the same original dataset.

Future work includes extending the motion primitive framework to tasks from real surgical procedures. Our standardized set of context and motion primitive labels can support skill analysis, error detection, and surgical automation. The proposed LOTO cross-validation method enables the assessment of models in generalizing across different surgical tasks and robots.

ACKNOWLEDGMENT

This work was partially supported by the Engineering-in-Medicine center at the University of Virginia and by the National Science Foundation under Grant No. 1842490 and 2146295. We thank the volunteer labelers and Dr. Schenkman, Dr. Cantrell, and Dr. Chen for their medical feedback.

REFERENCES

- [1] Ahmidi, N., Tao, L., Sefati, S., Gao, Y., Lea, C., Haro, B.B., Zappella, L., Khudanpur, S., Vidal, R., Hager, G.D.: A dataset and benchmarks for segmentation and recognition of gestures in robotic surgery. *IEEE Transactions on Biomedical Engineering* **64**(9), 2025–2041 (2017)
- [2] Allan, M., Kondo, S., Bodenstedt, S., Leger, S., Kadhodamohammadi, R., Luengo, I., Fuentes, F., Flouty, E., Mohammed, A., Pedersen, M., et al.: 2018 robotic scene segmentation challenge. *arXiv preprint arXiv:2001.11190* (2020)
- [3] Allan, M., Shvets, A., Kurmann, T., Zhang, Z., Duggal, R., Su, Y.H., Rieke, N., Laina, I., Kalavakonda, N., Bodenstedt, S., et al.: 2017 robotic instrument segmentation challenge. *arXiv preprint arXiv:1902.06426* (2019)
- [4] van Amsterdam, B., Clarkson, M., Stoyanov, D.: Gesture recognition in robotic surgery: a review. *IEEE Transactions on Biomedical Engineering* (2021)
- [5] van Amsterdam, B., Clarkson, M.J., Stoyanov, D.: Multi-task recurrent neural network for surgical gesture recognition and progress prediction. In: *2020 IEEE International Conference on Robotics and Automation (ICRA)*. pp. 1380–1386. IEEE (2020)
- [6] Boehm, J.R., Fey, N.P., Fey, A.M.: Online recognition of bimanual coordination provides important context for movement data in bimanual teleoperated robots. In: *2021 IEEE/RSJ International Conference on Intelligent Robots and Systems (IROS)*. pp. 6248–6255. IEEE (2021)
- [7] Bowyer, S.A., Davies, B.L., y Baena, F.R.: Active constraints/virtual fixtures: A survey. *IEEE Transactions on Robotics* **30**(1), 138–157 (2013)
- [8] De Rossi, G., Minelli, M., Roin, S., Falezza, F., Sozzi, A., Ferraguti, F., Setti, F., Bonfè, M., Secchi, C., Muradore, R.: A first evaluation of a multi-modal learning system to control surgical assistant robots via action segmentation. *IEEE Transactions on Medical Robotics and Bionics* (2021)
- [9] DiPietro, R., Ahmidi, N., Malpani, A., Waldram, M., Lee, G.I., Lee, M.R., Vedula, S.S., Hager, G.D.: Segmenting and classifying activities in robot-assisted surgery with recurrent neural networks. *International journal of computer assisted radiology and surgery* **14**(11), 2005–2020 (2019)
- [10] Falezza, F., Piccinelli, N., De Rossi, G., Roberti, A., Kronreif, G., Setti, F., Fiorini, P., Muradore, R.: Modeling of surgical procedures using statecharts for semi-autonomous robotic surgery. *IEEE Transactions on Medical Robotics and Bionics* **3**(4), 888–899 (2021)

TABLE VII: Datasets and definitions for gesture recognition

Paper	Dataset	Tasks	Gestures
Gao 2014 [12] [1]	JIGSAWS <ul style="list-style-type: none"> • Video • Kinematics 	Suturing Needle Passing Knot Tying	G1 - Reaching for needle with right hand G2 - Positioning needle G3 - Pushing needle through tissue G4 - Transferring needle from left to right G5 - Moving to center with needle in grip G6 - Pulling suture with left hand G7 - Pulling suture with right hand G8 - Orienting needle G9 - Using right hand to help tighten suture G10 - Loosening more suture G11 - Dropping suture at end and moving to end points G12 - Reaching for needle with left hand G13 - Making C loop around right hand G14 - Reaching for suture with right hand G15 - Pulling suture with both hands
DiPietro 2019 [9]	JIGSAWS MISTIC-SL <ul style="list-style-type: none"> • Video • Kinematics 	Suturing Needle Passing Knot Tying	G1-G12 & G14 G13 - Grab suture using 2nd needle driver G15 - Rotate suture twice using 1st needle driver around 2nd needle driver G16 - Grab suture tail using 2nd needle driver in knot tying G17 - Pull suture tail using 2nd needle driver through knot G18 - Pull ends of suture taut G19 - Rotate suture once using 2nd needle driver around 1st needle driver G20 - Grab suture tail using 1st needle driver in knot tying G21 - Pull suture tail using 1st needle driver through knot G22 - Grab suture using 1st needle driver
Gonzalez 2020 [17]	DESK <ul style="list-style-type: none"> • Video • Kinematics 	Peg Transfer	S1 - Approach peg S2 - Align & grasp S3 - Life peg S4 - Transfer peg - Get together S5 - Transfer peg - Exchange S6 - Approach pole S7 - Align & place
Menegozzo 2019 [30]	V-RASTED <ul style="list-style-type: none"> • Video • Kinematics 	Pick and Place	1 - Collecting ring 2 - Passing ring R to L 3 - Posing ring on pole 4 - Failing 1 5 - Failing 2 6 - Failing 3
Goldbraikh 2022 [16]	own <ul style="list-style-type: none"> • Video • Kinematics 	Suturing (not robotic)	No gesture Needle passing Pull the suture Instrument tie Lay the knot Cut the suture

- [11] Forestier, G., Lalys, F., Riffaud, L., Trelhu, B., Jannin, P.: Classification of surgical processes using dynamic time warping. *Journal of biomedical informatics* **45**(2), 255–264 (2012)
- [12] Gao, Y., Vedula, S.S., Reiley, C.E., Ahmidi, N., Varadarajan, B., Lin, H.C., Tao, L., Zappella, L., Béjar, B., Yuh, D.D., et al.: Jhu-isi gesture and skill assessment working set (jigsaws): A surgical activity dataset for human motion modeling. In: *MICCAI Workshop: M2CAI*. vol. 3, p. 3 (2014)
- [13] Ginesi, M., Meli, D., Roberti, A., Sansonetto, N., Fiorini, P.: Autonomous task planning and situation awareness in robotic surgery. In: *2020 IEEE/RSJ International Conference on Intelligent Robots and Systems (IROS)*. pp. 3144–3150. IEEE (2020)
- [14] Ginesi, M., Sansonetto, N., Fiorini, P.: Dmp++: Overcoming some drawbacks of dynamic movement primitives. *arXiv preprint arXiv:1908.10608* (2019)
- [15] Ginesi, M., Sansonetto, N., Fiorini, P.: Overcoming some drawbacks of dynamic movement primitives. *Robotics and Autonomous Systems* **144**, 103844 (2021)
- [16] Goldbraikh, A., Volk, T., Pugh, C.M., Laufer, S.: Using open surgery simulation kinematic data for tool and gesture recognition. *International Journal of Computer Assisted Radiology and Surgery* pp. 1–15 (2022)
- [17] Gonzalez, G.T., Kaur, U., Rahma, M., Venkatesh, V., Sanchez, N., Hager, G., Xue, Y., Voyles, R., Wachs, J.: From the desk (dexterous surgical skill) to the battlefield—a robotics exploratory study. *arXiv preprint arXiv:2011.15100* (2020)
- [18] Hughes, J.: krippendorffsalpha: An r package for measuring agreement using krippendorff’s alpha coefficient. *arXiv preprint arXiv:2103.12170* (2021)
- [19] Hutchinson, K., Li, Z., Cantrell, L.A., Schenkman, N.S., Alemzadeh, H.: Analysis of executional and procedural errors in dry-lab robotic surgery experiments. *The International Journal of Medical Robotics and Computer Assisted Surgery* **18**(3), e2375 (2022)
- [20] Kingma, D.P., Ba, J.: Adam: A method for stochastic optimization. *arXiv preprint arXiv:1412.6980* (2014)
- [21] Kitaguchi, D., Takeshita, N., Hasegawa, H., Ito, M.: Artificial intelligence-based computer vision in surgery: Recent advances and future perspectives. *Annals of Gastroenterological Surgery* **6** (10 2021). <https://doi.org/10.1002/ags3.12513>
- [22] Lalys, F., Jannin, P.: Surgical process modelling: a review. *International journal of computer assisted radiology and surgery* **9**(3), 495–511 (2014)
- [23] Lea, C., Hager, G.D., Vidal, R.: An improved model for segmentation and recognition of fine-grained activities with application to surgical training tasks. In: *2015 IEEE winter conference on applications of computer vision*. pp. 1123–1129. IEEE (2015)
- [24] Lea, C., Vidal, R., Reiter, A., Hager, G.D.: Temporal convolutional networks: A unified approach to action segmentation. In: *European Conference on Computer Vision*. pp. 47–54. Springer (2016)
- [25] Li, L., Li, X., Ding, S., Fang, Z., Xu, M., Ren, H., Yang, S.: Sirmet: Fine-grained surgical interaction recognition. *IEEE Robotics and Automation Letters* (2022)
- [26] Li, Z., Hutchinson, K., Alemzadeh, H.: Runtime detection of executional errors in robot-assisted surgery. In: *2022 International Conference on Robotics and Automation (ICRA)*. p. 3850–3856. IEEE Press (2022). <https://doi.org/10.1109/ICRA46639.2022.9812034>, <https://doi.org/10.1109/ICRA46639.2022.9812034>
- [27] Lin, H.C.: Structure in surgical motion. The Johns Hopkins University (2010)
- [28] Ma, R., Vanstrum, E.B., Nguyen, J.H., Chen, A., Chen, J., Hung, A.J.: A novel dissection gesture classification to characterize robotic dissection technique for renal hilar dissection. *The Journal of Urology* **205**(1), 271–275 (2021)
- [29] Meli, D., Fiorini, P.: Unsupervised identification of surgical robotic actions from small non homogeneous datasets. *arXiv preprint arXiv:2105.08488* (2021)
- [30] Menegozzo, G., Dall’Alba, D., Zandonà, C., Fiorini, P.: Surgical gesture recognition with time delay neural network based on kinematic data. In: *2019 International Symposium on Medical Robotics (ISMR)*. pp. 1–7. IEEE (2019)
- [31] Neumuth, D., Loebe, F., Herre, H., Neumuth, T.: Modeling surgical processes: A four-level translational approach. *Artificial intelligence in medicine* **51**(3), 147–161 (2011)
- [32] Nwoye, C.I., Yu, T., Gonzalez, C., Seeliger, B., Mascagni, P., Mutter,

TABLE VIII: Datasets and models for surgical actions

Paper	Dataset	Tasks	Actions
Nwoye 2022 [32]	CholecT50 • Video	Laparoscopic cholecystectomy	Aspirate Clip Coagulate Cut Dissect Grasp Irrigate Null Pack Retract
Li 2022 [25]	EndoVis2018 • Video	Nephrectomy	Cauterization Suction Staple Ultrasound sensing Looping Idle Tool manipulation Suturing Clipping Retraction
Meli 2021 [29]	own • Video • Kinematics	Ring Transfer	Move Grasp Release Extract
Forestier 2012 [11]	own • Video	Lumbar disk herniation	Right: Sew Install Hold Remove Coagulate Swab Irrigate Left: Hold Install Remove
Wagner 2021 [42]	EndoVis 2019 • Video	Laparoscopic cholecystectomy	Grasp Hold Cut Clip
De Rossi 2021 [8]	own • Video	Pick and place (semi-autonomous and cooperative)	A01 – MS moves to ring A02 – MS picks ring A03 – MS moves ring to exchange area A04 – AS moves to ring A05 – AS grasps ring and MS leaves ring A06 – AS moves ring to delivery area A07 – AS drops ring on target A08 – AS moves to starting position
Valderrama 2022 [40]	PSI-AVA • Video	Radical prostatectomy	Cauterize Close Close Something Cut Grasp Hold Open Open Something Pull Push Release Staple Still Suction Travel Wash
Ma 2021 [28]	own • Video	Renal hilum dissection (Partial nephrectomy)	Single blunt dissection: Spread Peel/push Hook Single sharp dissection: Cold cut Hot cut Burn dissect Combination: Pedicalize 2-hand spread Coagulate then cut

- D., Marescaux, J., Padoy, N.: Rendezvous: Attention mechanisms for the recognition of surgical action triplets in endoscopic videos. *Medical Image Analysis* **78**, 102433 (2022)
- [33] Park, S., Mohammadi, G., Artstein, R., Morency, L.P.: Crowdsourcing micro-level multimedia annotations: The challenges of evaluation and interface. In: *Proceedings of the ACM multimedia 2012 workshop on Crowdsourcing for multimedia*. pp. 29–34 (2012)
- [34] Paszke, A., Gross, S., Massa, F., Lerer, A., Bradbury, J., Chanan, G., Killeen, T., Lin, Z., Gimelshein, N., Antiga, L., et al.: Pytorch: An imperative style, high-performance deep learning library. *Advances in neural information processing systems* **32** (2019)
- [35] Rivas-Blanco, I., Pérez-del Pulgar, C.J., Mariani, A., Quaglia, C., Tortora, G., Mencias, A., Muñoz, V.F.: A surgical dataset from the da vinci research kit for task automation and recognition. *arXiv preprint arXiv:2102.03643* (2021)
- [36] Sefati, S., Cowan, N.J., Vidal, R.: Learning shared, discriminative dictionaries for surgical gesture segmentation and classification. In: *MICCAI Workshop: M2CAI*. vol. 4 (2015)
- [37] Sutherland, G.R., Maddahi, Y., Gan, L.S., Lama, S., Zareinia, K.: Robotics in the neurosurgical treatment of glioma. *Surgical Neurology International* **6**(Suppl 1), S1 (2015)
- [38] Tao, L., Elhamifar, E., Khudanpur, S., Hager, G.D., Vidal, R.: Sparse hidden markov models for surgical gesture classification and skill evaluation. In: *International conference on information processing in computer-assisted interventions*. pp. 167–177. Springer (2012)
- [39] Twinanda, A.P., Shehata, S., Mutter, D., Marescaux, J., De Mathelin, M., Padoy, N.: Endonet: a deep architecture for recognition tasks on laparoscopic videos. *IEEE transactions on medical imaging* **36**(1), 86–97 (2016)
- [40] Valderrama, N., Ruiz Puentes, P., Hernández, I., Ayobi, N., Verlyck, M., Santander, J., Caicedo, J., Fernández, N., Arbeláez, P.: Towards holistic surgical scene understanding. In: *International Conference on Medical Image Computing and Computer-Assisted Intervention*. pp. 442–452. Springer (2022)
- [41] Varadarajan, B., Reiley, C., Lin, H., Khudanpur, S., Hager, G.: Data-derived models for segmentation with application to surgical assessment and training. In: *International Conference on Medical Image Computing and Computer-Assisted Intervention*. pp. 426–434. Springer (2009)
- [42] Wagner, M., Müller-Stich, B.P., Kisilenko, A., Tran, D., Heger, P., Mündermann, L., Lubotsky, D.M., Müller, B., Davitashvili, T., Capek, M., et al.: Comparative validation of machine learning algorithms for surgical workflow and skill analysis with the heichole benchmark. *arXiv preprint arXiv:2109.14956* (2021)
- [43] Wang, T., Jin, M., Li, M.: Towards accurate and interpretable surgical skill assessment: a video-based method for skill score prediction and guiding feedback generation. *International Journal of Computer Assisted Radiology and Surgery* pp. 1–11 (2021)
- [44] Ward, T.M., Hashimoto, D., Ban, Y., Witkowski, E.R., Lillemoe, K.D., Rosman, G., Meireles, O.R.: Training with pooled annotations from multiple surgeons has no effect on a deep learning artificial intelligence model’s performance. *J Am Coll Surg* **231**(4), e203 (2020)
- [45] Yasar, M.S., Alemzadeh, H.: Real-time context-aware detection of unsafe events in robot-assisted surgery. In: *2020 50th Annual IEEE/IFIP International Conference on Dependable Systems and Networks (DSN)*. pp. 385–397. IEEE (2020)
- [46] Yasar, M.S., Evans, D., Alemzadeh, H.: Context-aware monitoring in robotic surgery. In: *2019 International Symposium on Medical Robotics (ISMR)*. pp. 1–7. IEEE (2019)